

Reaction Pathways of Acetylene on Pd/W(211): A TPD and HREELS Investigation

Ihab M. Abdelrehim,[†] Kalman Pelhos, and Theodore E. Madey**Laboratory for Surface Modification, Department of Physics and Astronomy, Rutgers University, Piscataway, New Jersey 08854-8019*Joseph Eng, Jr. and Jingguang G. Chen^{*,‡}*Corporate Research Laboratories, Exxon Research and Engineering Company, Annandale, New Jersey 08801**Received: June 12, 1998; In Final Form: September 25, 1998*

In an ongoing investigation to study structure–reactivity relationships on bimetallic surfaces, acetylene cyclotrimerization to form benzene is of particular interest: in this structure-sensitive catalytic reaction, C–C and C–H bonds can be formed readily under ultrahigh vacuum (UHV) conditions without C–C bond breaking. In this paper, we present results for acetylene cyclization and hydrogenation on Pd/W(211). Pd on W is chosen because it is a morphologically unstable system, and W(211) facets develop after annealing Pd/W(111) to ≥ 700 K. Temperature-programmed desorption (TPD) results exhibit negligible amounts of benzene detected from acetylene adsorption on clean W(211). A single monolayer (ML) of Pd on W(211) decreases the high reactivity toward acetylene decomposition and several different reaction pathways are accessed, including hydrogenation of C_2H_2 to C_2H_4 and cyclotrimerization of C_2H_2 to form C_6H_6 . The cyclotrimerization reaction produces three benzene desorption states at ~ 340 , ~ 390 , and ~ 430 K. In addition, the detection of C_4H_6 during TPD provides evidence that an elusive C_4H_4 intermediate is present on the surface. Furthermore, ethylene is observed in substantial yields, lending insight into the activity of the bimetallic system. The use of high-resolution electron energy-loss spectroscopy (HREELS) provides complementary information regarding the reaction mechanisms of acetylene on the Pd/W(211) surfaces.

1. Introduction

In the companion paper, our focus has been on the surface chemistry of acetylene (C_2H_2) and benzene (C_6H_6) on clean and carbide-covered W(211) surfaces.¹ In the present paper, we report on the surface chemistry of acetylene on a W(211)-based bimetallic system, i.e., ultrathin Pd films on W(211). In contrast to the complete decomposition of acetylene seen on W(211),¹ a single monolayer (ML) of Pd on W(211) is found to be an effective catalyst for acetylene cyclization ($3C_2H_2 \rightarrow C_6H_6$) to form benzene and C_4H_6 , as well as an excellent catalyst in acetylene hydrogenation to form ethylene.

Acetylene cyclization (also called cyclotrimerization) is an important reaction that has been studied on a variety of single-crystal surfaces under ultrahigh vacuum (UHV) conditions for over a decade;^{2–33} for a recent survey of the literature, see ref 34. Bertolini et al. were the first to observe acetylene cyclization to benzene on supported Ni catalysts,³⁵ while the only reported acetylene cyclization studies on high-area Pd materials (i.e., actual catalytic turnovers) were performed by Ormerod and Lambert.³⁶ In addition, acetylene cyclization has been observed to occur under high-pressure conditions over Pd single-crystal surfaces¹⁰ as well as in homogeneous organometallic environments.^{11,12} The correlation between UHV, high-pressure, and organometallic investigations prompts further examination into the intricacies of this reaction. The motivation for studying acetylene cyclization under UHV conditions is its extreme

structure sensitivity. For instance, certain single-crystal surfaces such as Pd(111)^{2–10,13–22,25–28} and Cu(110)^{23,24} are highly selective toward cyclotrimerization of acetylene, whereas the reaction is much less selective on the Pd(110) surface.^{5,10} The specificity of this reaction to the surface conditions of well-ordered single crystals provides a distinct quality for probing the effects of surface electronic and geometric properties.

In addition to the numerous acetylene cyclization studies on elemental single-crystal metal surfaces,^{2–33} there have also been reports of acetylene cyclization studies on bimetallic surfaces^{37–43} and supported metals.^{35,36} Model bimetallic surfaces include Pd/Au(111),^{38,39} Au/Pd(111),⁴⁰ Pd/Mo(100),⁴¹ Pd/Ta(110),⁴² and Sn/Pt(111);⁴³ of these, the Pd/Au,^{38–40} Pd/Ta,⁴² and Sn/Pt⁴³ systems are the only bimetallics observed to catalyze the cyclization reaction. The highest selectivity toward cyclization has been observed on Pd/Au surfaces with catalytic efficiencies reaching $\sim 100\%$.^{39,40}

The hydrogenation of acetylene to form ethylene has been reported to occur concurrently with the cyclization reaction on single-crystal Pd surfaces.^{2,3,5,10,44} The Pd(111) surface is detected to be active toward acetylene hydrogenation.^{2,3,5,10} On the other hand, the Pd(110) surface shows reduced activity in the studies performed by Rucker et al.¹⁰ and has been observed to be relatively inactive toward ethylene formation by Gentle et al.⁵ and Yoshinobu et al.⁴⁴ These results support the belief that the specificity for acetylene hydrogenation to form ethylene is also driven by changes in the surface structure and morphology.

The remarkable efficiency of making C–C or C–H bonds under UHV conditions without undergoing C–C bond scission,

* To whom correspondence should be addressed.

[†] Present address: Evans East, Plainsboro, NJ 08536.[‡] Present address: University of Delaware, Department of Materials Science & Engineering, Newark, DE 19716.

as verified by isotopic studies,²⁵ is significant to the understanding of catalytic reaction pathways (i.e., acetylene cyclization to benzene or hydrogenation to form ethylene). Kinetic and mechanistic studies^{3,25–28} indicate that benzene formation on Pd(111) is a desorption rate-limited process. Furthermore, a number of investigations have focused on identifying the intermediates present during acetylene cyclotrimerization on Pd(111).^{3,14–19,27,31,45} Although much evidence points to the role of a C₄H₄ intermediate formed by coupling two C₂H₂ species, the only direct evidence for the presence of C₄H₄ in acetylene cyclization on Pd(111) is based on molecular beam³ and LITD/FTMS^{27,28} measurements.

The goal of this paper is to amplify a previous preliminary report³⁴ and present new results for acetylene cyclization and hydrogenation over a bimetallic surface (Pd/W(211)). The surface and interface properties of bimetallic and alloy systems have been the subject of many investigations because of their unique physical and chemical properties.^{46,47} The driving force for the present study is the morphological instability of ultrathin metal films deposited on refractory metals.^{48,49} For instance, atomically rough bcc W(111) and Mo(111) coated with a single monolayer of certain metals (Pt, Pd, Ir, Rh, Au) undergo massive reconstruction to form highly faceted surfaces upon annealing to ≥ 700 K.^{48,50,51} Pyramidal facets consisting of faces with {211} orientation and nanometer-scale dimensions are observed when ≥ 1 ML Pd/W(111) is heated above 700 K.^{49,50,52}

Butane hydrogenolysis investigations on Pt/W(111) have shown that the planar surface has a higher selectivity toward ethane production and higher reaction rates, while methane formation is dominant on the faceted surface.⁵³ In addition, increasing facet size decreases the concentration of 4-fold coordination (C₄) sites, which correlates with reduced ethane production.⁵³ These studies suggest that the catalytic activity and production of intermediates responsible for product formation are affected by surface morphology. To study the structure–reactivity relationship of the morphologically unstable Pd/W system further, acetylene cyclization, a known structure-sensitive process, has been chosen as a probing reaction in the current study.

The surface geometrical structure of clean W(211) is similar (but not identical) to that of an fcc(110) row/trough type configuration. One physical monolayer of Pd grows pseudomorphically on W(112) and adopts the row/trough configuration of the substrate.⁴⁹ Previous investigations have shown little or no acetylene converts to ethylene on Pd(110).^{5,10,44} Furthermore, since little or no conversion of acetylene to benzene is observed on Pd(110) whereas Cu(110) has $\sim 85\%$ selectivity to benzene formation,²⁴ it is of interest to see if the Pd/W bimetallic system can catalyze the cyclotrimerization reaction. More specifically, the use of W(211) maintains the row-and-trough-type geometry while our goal is to determine whether vapor-depositing thin films of Pd perturbs the electronic structures of both metals sufficiently to enhance the reactivity toward cyclotrimerization and hydrogenation. In addition, it is of interest to determine if the C₄H₄ intermediate believed to be present on hexagonal substrates (e.g., Pd(111), Sn/Pt(111), etc.) is also seen on surfaces of different symmetry. In our studies we examine the cyclization and hydrogenation reactions of acetylene on Pd films with a thickness ranging from a monolayer to multilayers deposited on a W(211) surface. Note that the palladium/tungsten surface is not believed to form an alloy at monolayer Pd coverages, as indicated by low-energy ion scattering (LEIS) studies of Pd/W(111).⁵⁴ As demonstrated below, TPD and

HREELS results clearly reveal the different reaction pathways for acetylene on clean W(211) as compared to Pd/W(211).

2. Experimental Section

TPD experiments have been performed at Rutgers in a previously described UHV chamber with a base pressure of 1×10^{-10} Torr,⁴⁸ while the HREELS investigations have been performed at the Exxon Corporate Research Laboratories in a UHV system with a base pressure of 2×10^{-10} Torr.⁵⁵ The chambers are equipped with low-energy electron diffraction (LEED), an Auger electron spectrometer (AES), and a quadrupole mass spectrometer (QMS) used for monitoring background residual gas and detecting desorbed species during TPD. The details of the HREEL spectrometer are discussed in the companion paper.¹ Briefly, The HREEL spectra reported here have a spectroscopic resolution (full-width at half-maximum) of 30–40 cm⁻¹ and an elastic peak intensity ranging from 10⁵ to 10⁶ cps. HREEL spectra were taken in the on-specular and -15° off-specular directions.

The W(211) sample is ~ 8 mm in diameter and aligned within 0.5° of the (211) plane. The surface is spot welded to tantalum leads for support and resistive heating. At Rutgers, the sample could be cryogenically cooled to ~ 100 K and resistively heated to 1300 K and during cleaning it could be heated by electron bombardment to 2400 K, as measured using a W-5%Re/W-26%Re thermocouple junction. At Exxon, a type K thermocouple was used as a consequence of sample temperatures not exceeding 1200 K, due to different cleaning procedures. The Exxon chamber also has liquid-nitrogen cooling capabilities.

The preparation of the surface differs between the Rutgers and Exxon chambers. The Exxon surface preparation involves cycles of sputtering and annealing, as discussed in the companion paper.¹ At Rutgers the surface is cleaned by annealing at 1200 K in 5×10^{-8} Torr of oxygen for 1–5 min to remove residual carbon, followed by flashing to 2400 K (heating rate $\cong 400$ K/s) to remove metal overlayers as well as chemisorbed oxygen. Preparation of the Pd films is similar in the TPD and HREELS studies. The bimetallic surfaces prepared prior to TPD experimentation at Rutgers are preannealed to 700 or 1050 K by heating from 100 to 700 K (1050 K) at 5 K/s, cooling to 100 K, and dosing with acetylene. The desorption yield for a reaction product is proportional to the corrected integrated peak area of a TPD spectrum for that desorption product. For the HREELS experiments, all of the surfaces are preannealed by heating to 700 K ($\beta = 5$ K/s), holding for 1 min, cooling, and then dosing with acetylene. The preannealing to 700 K serves two functions: to order the surface overlayer and to cause desorption of hydrogen, CO, etc. which may have adsorbed during Pd deposition. In the following text, we refer to these surfaces as 700 K preannealed and 1050 K preannealed ~ 1 ML Pd/W(211) or ~ 6 ML Pd/W(211). The surface cleanliness and long-range order have been verified by AES and LEED, respectively.

The spectral-grade acetylene (99.96% pure) has been purified with a dry ice/acetone cooled trap. The purity is checked with mass spectrometry prior to and during use in the UHV chambers. A glass flask with 1 atm of deuterated acetylene (99.9% atomic purity) was purchased prepurified. All acetylene dosing is performed using a sapphire-sealed variable leak valve with the surface temperature maintained at ~ 100 K. Acetylene exposures are not corrected for ion gauge sensitivities.

The metal evaporation sources at both Rutgers and Exxon consist of high-purity Pd wire wrapped around a larger diameter W wire (~ 0.25 mm diameter). Metal evaporation rates are

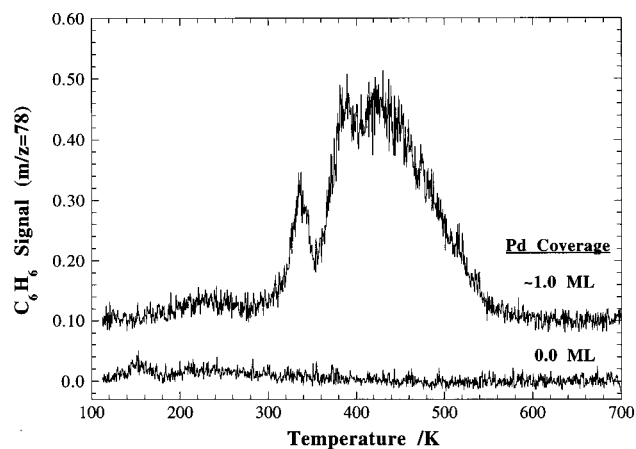


Figure 1. TPD spectra of reactively formed benzene ($m/z = 78$) from 3 L of acetylene on clean W(211) and ~ 1.0 ML Pd/W(211) preannealed to 700 K. The heating rate is 5 K/s.

controlled by varying the current used to resistively heat the wire. In addition, the evaporation source is outgassed extensively prior to deposition. The purity of the Pd overlayers on W(211) is always confirmed by AES prior to reaction experiments.

3. Results and Discussion

3.1. TPD Studies. The initial phase of our TPD studies has involved the use of a multiplexing technique to identify the dominant desorption products (in the temperature range from ~ 100 to 700 K) following adsorption of C_2H_2 on Pd/W(211). In this way, it is found that the dominant species include C_6H_6 (benzene) as well as C_4H_x and C_2H_y products. Consequently, the TPD results presented here include data for benzene ($m/z = 78$, $C_6H_6^+$), the main product expected from the cyclization of acetylene, as well as ethylene (monitored by observing $m/z = 27$, $C_2H_3^+$), a hydrogenation product of acetylene. In addition, $C_4H_6^+$ ($m/z = 54$), a hydrogenated form of a possible C_4H_x intermediate, was also measured; its presence during the formation of benzene is crucial to a mechanistic understanding of the cyclization reaction. To study the desorption profile of the possible C_4H_x intermediate, the $C_4H_6^+$ ($m/z = 54$) fragment is monitored rather than $C_4H_4^+$ ($m/z = 52$) to avoid interference from cracking of product benzene ($m/z = 54$ is insignificant in the cracking pattern of benzene, whereas $m/z = 52$ is relatively intense).

Figure 1 shows TPD spectra of benzene following the adsorption of 3 L of acetylene at 100 K on clean and ~ 1 ML Pd/W(211). The clean W(211) surface measurements show trace amounts of benzene desorbing from the surface. In contrast, on the ~ 1 ML Pd/W(211) surface, acetylene reacts to form benzene in significant quantities (~ 6 –8% of a saturation coverage of acetylene is converted to benzene). The dominant TPD features for reactively formed benzene appear at ~ 430 and ~ 390 K with a smaller peak at ~ 340 K; the spectra are similar to those reported earlier except for minor differences at low temperature.³⁴ In previous studies, a high-temperature desorption peak (~ 480 –500 K) has been attributed to a flat-lying species on the Pd(111) surface.^{2–6,22}

Figures 2 and 3 demonstrate the detection of a $C_4H_6^+$ species during TPD following adsorption of C_2H_2 . Previously, the only reported TPD observations of $C_4H_6^+$ from thermally desorbed, reactively formed C_4H_6 were for a Sn/Pt(111) surface⁴³ and for reduced $TiO_2(001)$.⁵⁶ The desorption of a C_4H_x intermediate from Pd(111) was observed only during molecular-beam³ or

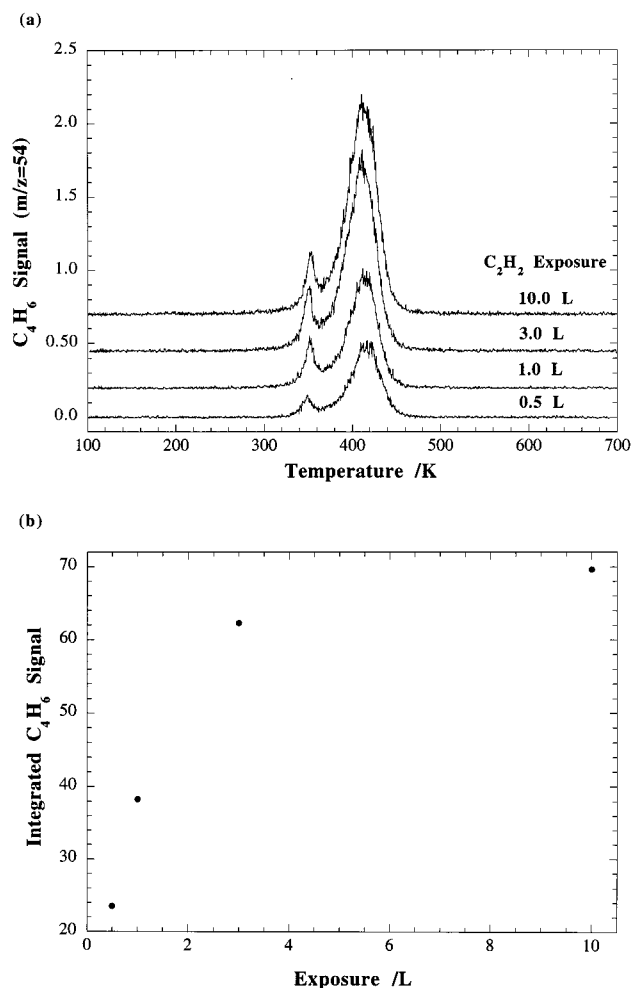


Figure 2. (a) TPD spectra of reactively formed C_4H_6 ($m/z = 54$) from several acetylene exposures on a 700 K preannealed ~ 1.0 ML Pd/W(211). (b) Integrated C_4H_6 peak areas for TPD spectra shown in (a).

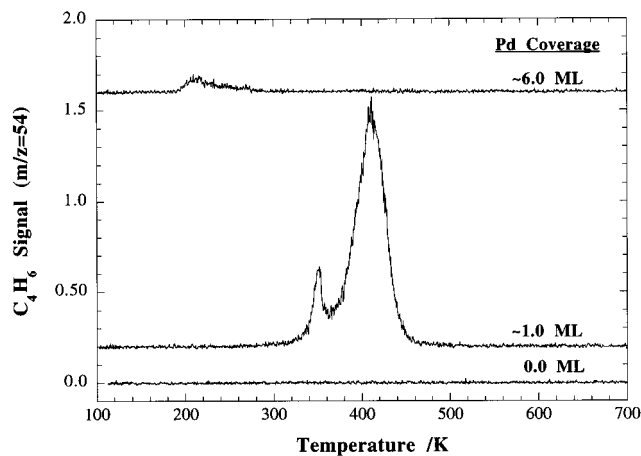


Figure 3. TPD spectra of reactively formed C_4H_6 from 3 L of acetylene on 700 K preannealed clean W(211) and ~ 1 and ~ 6 ML Pd/W(211).

LITD^{27,28} measurements. The observation of the elusive $C_4H_6^+$ species indicates that Pd/W(211) is an interesting bimetallic system to probe. Figure 2a illustrates the effects of increasing the exposure of acetylene from 0.5 to 10 L on a preannealed (700 K) ~ 1 ML Pd/W(211). As the acetylene exposure is increased, the $C_4H_6^+$ yield increases and saturates above 3–4 L exposure of acetylene (Figure 2b). The saturation level for reactively formed benzene also occurs above ~ 3 –4 L of acetylene (Figure 1 and ref 34). The 420 K feature in Figure

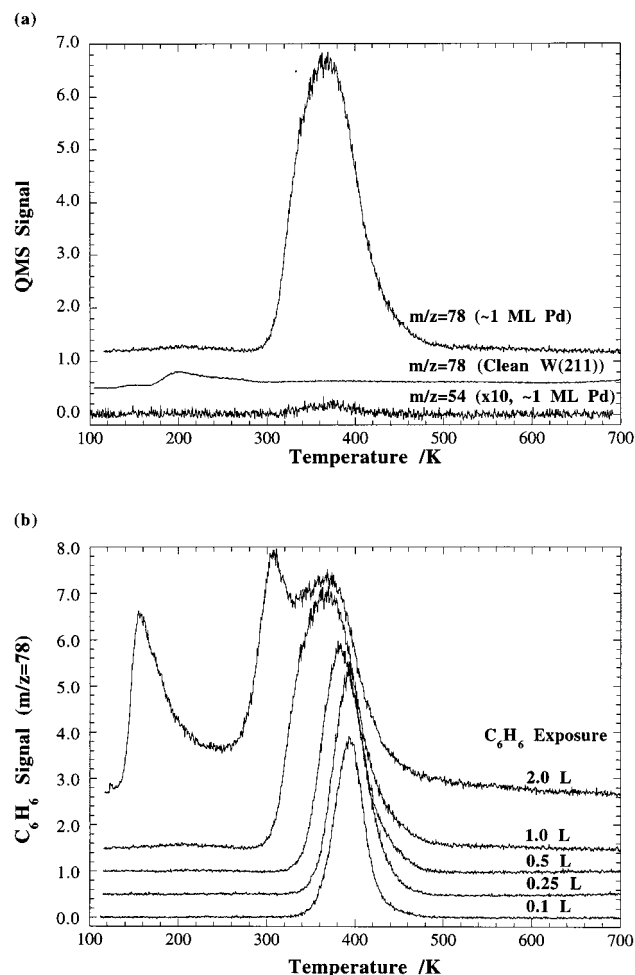


Figure 4. (a) C_6H_6 and C_4H_6 desorption spectra from molecular chemisorption of 1 L of benzene on clean W(211) and ~1 ML Pd/W(211) preannealed to 700 K. (b) TPD of benzene from several exposures of molecular benzene (0.1–2.0 L).

2a is almost coincident with the high-temperature benzene desorption peak (430 K), while the 340 K feature is almost coincident with the benzene desorption state at 340 K. The comparison of clean W(211) (where no reaction is observed) to a 700 K preannealed ~1 ML Pd/W(211) demonstrates a remarkable change in the activity of the substrate to C_4H_6 formation (Figure 3). An increase in the Pd coverage to ~6 ML Pd greatly reduces the activity of the surface for this reaction, resulting in minute amounts of C_4H_6 observed during TPD (Figure 3). The near absence of C_4H_6 product from this surface is related to the fact that the W(211) substrate is covered by a polycrystalline Pd film ~6 ML thick.

To ascertain whether the reactively formed benzene is reaction-rate-limited or desorption-rate-limited, TPD experiments have also been performed following adsorption of benzene (Figure 4). Figure 4a shows the desorption of benzene ($m/z = 78$) after dosing 1 L of benzene onto both a clean W(211) surface and ~1 ML Pd/W substrate, each of which is preannealed to 700 K. The adsorption of 1 L of benzene on clean W(211) shows little C_6H_6 desorption, indicating that complete decomposition is highly favored (Figure 4a). A strong benzene desorption feature is detected at 370 K for ~1 ML Pd/W(211) (Figure 4a) and appears at a temperature ~60–70 K below the main feature seen with reactively formed benzene in Figure 1. In addition, previous HREELS measurements of acetylene adsorbed on ~1 ML Pd/W(211) did not detect the formation of benzene when the surface was heated to 400 K.³⁴ This is a

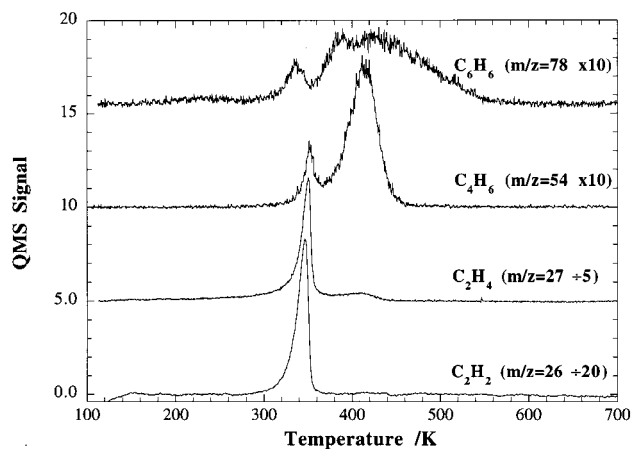


Figure 5. TPD spectra of acetylene (C_2H_2) along with cyclization (C_6H_6 , C_4H_6) and hydrogenation products (C_2H_4) from 3 L of acetylene on 700 K preannealed ~1 ML Pd/W(211).

strong indication that desorption of reactively formed benzene is reaction-rate-limited. At chemisorbed benzene exposures >1 L (Figure 4b), a 310 K peak appears and saturates with a magnitude similar to that of the 400 K feature. In addition, the 150 K peak continues to grow without saturating, even with a 10 L benzene exposure (not shown), indicating an increased concentration of a weakly bound benzene species caused by a condensed multilayer. In addition to benzene, $C_4H_6^+$ is also monitored in order to establish whether the C_4H_x species is associated with chemisorbed benzene reactions (Figure 4a). The insignificant amounts of C_4H_6 ($m/z = 54$) observed in Figure 4a demonstrate that C_4H_x is not a fragment nor a product resulting from benzene decomposition.

In determining product yields from TPD data, the hydrocarbon signals are corrected using their corresponding ionization sensitivities;⁵⁷ since ionization sensitivities for C_4H_6 have not been found, the ionization efficiencies for C_4H_8 are used in this work.⁵⁷ The QMS is calibrated against a nude Bayard–Alpert gauge using calibrant gases (C_2H_2 , C_2H_4 , and C_6H_6). Since C_4H_6 has several isomers and we have not identified which isomer is desorbing, we assume that the QMS transmission and detection efficiencies are the same for both C_4H_6 and C_6H_6 . The relative intensities of the various desorption products following adsorption of C_2H_2 are estimated by comparing several product spectra formed from the adsorbed acetylene on preannealed ~1 ML Pd/W(211) (Figure 5). The relative intensities of the $C_6H_6^+$ and $C_4H_6^+$ reaction product peaks from 3 L of acetylene are not characteristic of C_6H_6 formation, verifying that C_4H_6 is definitely not a fragment of benzene (note the very low $m/z = 54$ (C_4H_6) intensity in the molecular benzene experiments shown in Figure 4a). In addition, the common features at ~340 and 420 K in the benzene and C_4H_6 TPD spectra are also consistent with the involvement of a C_4H_4 intermediate in the reaction pathway of benzene formation. Moreover, as shown in Figures 5 and 6 and discussed below, the TPD peak intensities of ethylene are much greater than those of benzene or C_4H_6 , indicating that the pathway toward acetylene hydrogenation is favored on the ~1 ML Pd/W(211) surface.

The hydrocarbon yields from the saturation coverage of acetylene adsorbed on the 700 K preannealed ~1 ML Pd/W(211) surface have been estimated based on the relative peak areas in Figure 5. About 57% of the adsorbed C_2H_2 reacts to form products: 45% of the C_2H_2 is converted to ethylene, ~12% of the C_2H_2 is converted to cyclization products ($C_6H_6^+$ and $C_4H_6^+$), while the remaining C_2H_2 desorbs intact; we suggest

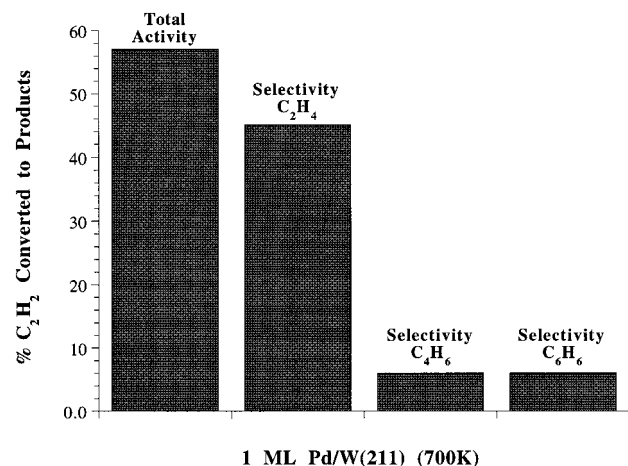
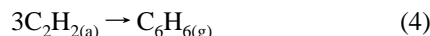
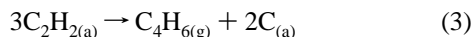
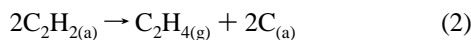
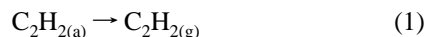


Figure 6. Histogram showing the total activity toward product formation, as well as the selectivity to C_2H_4 , C_4H_6 , and C_6H_6 formation from a saturation coverage of acetylene on a 700 K preannealed ~ 1 ML Pd/W(211) surface.

that the desorption and decomposition of acetylene take place via the following reactions:



The hydrocarbon yields have been corrected as described above and calculated with respect to a saturation coverage of acetylene and by assuming reaction pathways 1–4. These yields are used to plot a histogram of activity and selectivity for a saturation coverage of C_2H_2 on ~ 1 ML Pd/W(211), as shown in Figure 6. Previously, Rucker et al. have observed ~ 13 – 15% conversion of acetylene to ethylene on Pd(111) and Pd(110),¹⁰ while other groups indicate no ethylene formation on the Pd(110) surface.^{5,44} The results presented here show at least 3 times more ethylene formation on the ~ 1 ML Pd/W substrate compared to previous results for Pd(110),^{5,10,44} indicating a high activity toward hydrogenation. Although our benzene yields on Pd/W(211) are comparable to those on Pd(110)¹⁰ and Sn/Pt(111),⁴³ the total cyclization products we observe are ~ 2 times higher, with the difference being the appearance of equivalent amounts of C_4H_6 . The manipulation of geometrical and electronic properties of the W substrate accompanying the deposition of ~ 1 ML Pd has resulted in a different outcome for several reaction pathways and product yields (in comparison with Pd(110)¹⁰ and Sn/Pt(111)⁴³), particularly for the case of ethylene production.

Increasing the Pd film thickness causes large changes in ethylene and benzene product distributions formed from 3L of acetylene (see Figure 7). Benzene yields from 3 L of acetylene decrease by a factor of 50% on a 700 K preannealed ~ 6 ML Pd/W substrate in comparison to the ~ 1 ML Pd/W 700 K preannealed surface (Figure 7a), indicating a decreased activity toward benzene formation or the presence of a subsequent decomposition pathway for reactively formed benzene. The HREELS investigations presented below (section 3.2.1) show evidence for the presence of surface benzene and provide support for the decomposition pathway. On the other hand, heating the ~ 6 ML Pd/W surface to 1050 K results in a significant increase in the benzene yield (~ 5 -fold increase); the

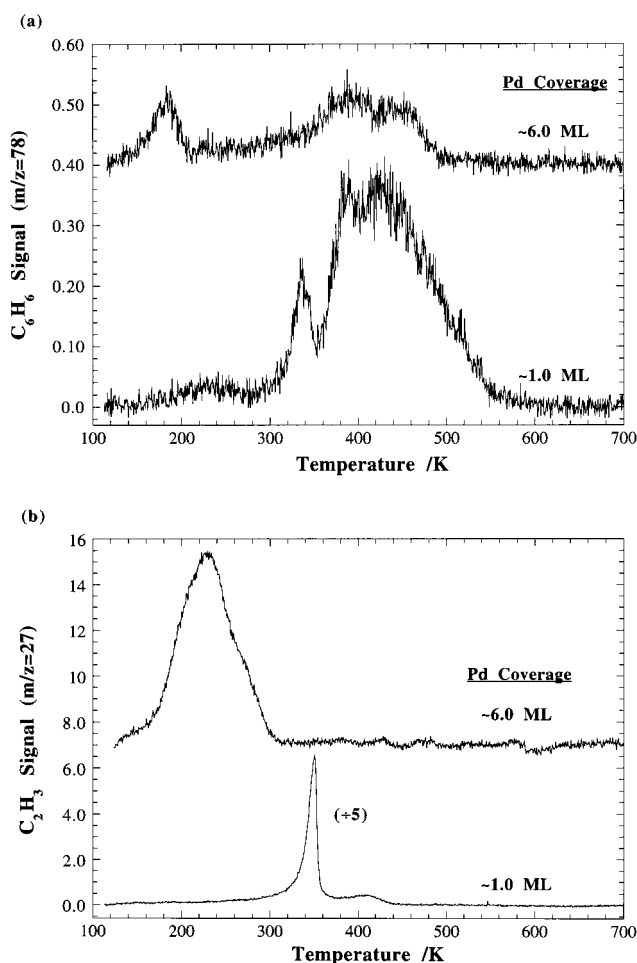


Figure 7. TPD spectra of reactively formed (a) benzene and (b) ethylene on 700 K preannealed ~ 1 and ~ 6 ML Pd/W(211).

details of these results are not shown and will be presented in a subsequent paper.⁵⁸ In addition, the chemisorption of 1 L of benzene on 700 K preannealed ~ 6 ML Pd/W(211), followed by thermal desorption (not shown), reveals that the benzene yield is equivalent to the amount observed with reactively formed benzene on the same substrate (Figure 7a); this observation indicates that both adsorption and formation of C_6H_6 are limited by the surface density of adsorption or reaction sites on the thick Pd/W(211) film. In addition, ethylene desorption temperatures are lower (~ 220 K) on the 700 K preannealed ~ 6 ML Pd/W(211) surface as opposed to the ~ 1 ML Pd/W(211) substrate (Figure 7b). However, ethylene yields on a 700 K preannealed ~ 1 and ~ 6 ML Pd/W surface are equivalent. Hence, the surface properties of ~ 6 ML Pd/W(211) may be causing weaker metal–adsorbate interactions resulting in lower desorption temperatures while leaving yields unchanged for reactively formed ethylene.

In Figure 8 we plot the relative yields of benzene and C_4H_6 ; in each case, the integrated yield on the ~ 1 ML Pd/W(211) surface is compared with that on the ~ 6 ML Pd/W(211) surface. The TPD peak area of C_4H_6 is reduced on the 700 K preannealed ~ 6 ML Pd/W(211) film (see Figure 8) in correspondence with the reduction in yield of reactively formed benzene (cf. Figures 7a and 8). However, the HREELS data presented in section 3.2.1 suggests that a C_4H_4 intermediate is present on the ~ 6 ML Pd/W surface after heating to 300 K and that a majority of the C_4H_x intermediate converts to form surface benzene, which subsequently desorbs or decomposes. On the basis of AES and STM,⁵⁹ we believe the ~ 6 ML Pd film is continuous, i.e.,

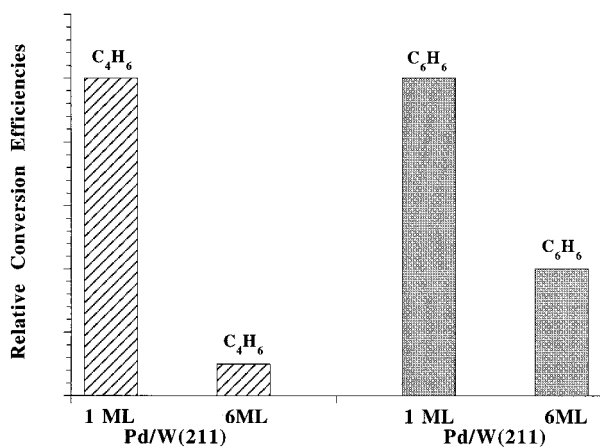


Figure 8. Histogram showing the relative conversion efficiencies of C_4H_6 and C_6H_6 on a ~ 1 and ~ 6 ML Pd/W(211) surface preannealed to 700 K.

covering the surface more-or-less uniformly at 700 K, but that it may undergo phase-separation into clusters and monolayer Pd when heated to 1050 K for several minutes; surface alloying of Pd and W also occurs when multilayer Pd films are annealed to 1050 K.⁵⁸ The changes observed on the 700 K preannealed thick Pd/W film and the lower temperature ethylene desorption may also be causing benzene formation to proceed at lower temperatures, as seen by the presence of surface benzene in the HREELS data (section 3.2.1). Since the measurements made over thick Pd films are mostly beyond the scope of the present paper, the results and detailed discussion of the multilayer investigations will be presented in a future manuscript.⁵⁸

3.2. HREELS Investigations. Having established the identity of the gas-phase reaction products in the previous section, we now attempt to identify the surface intermediates by using HREELS. The emphasis of this section is on identifying the surface intermediates present on the ~ 1 and ~ 6 ML Pd/W(211) surfaces; the surface intermediates formed on the clean W(211) are only briefly mentioned in this paper. A more detailed discussion of the C_2H_2 /W(211) chemistry can be found in the companion paper.¹

3.2.1. Acetylene on Clean W(211) and Pd/W(211). Figure 9 compares the HREEL spectra obtained after exposing a clean W(211) surface and a ~ 1 and ~ 6 ML Pd/W(211) surface to 1 L of acetylene at 100 K. Such a comparison reveals that acetylene interacts differently with each surface. For example, the spectrum of acetylene on clean W(211) (Figure 9a) is consistent with di- σ/π -bonded acetylene¹ but the spectrum of acetylene on the ~ 1 ML Pd/W(211) surface (Figure 9b) is consistent with a mixture of molecularly adsorbed acetylene and acetylide (CCH), as shown by the isotopic labeling studies discussed below. In the spectrum of acetylene on the ~ 6 ML Pd/W(211) surface (Figure 9c), the predominant species is molecular acetylene. The vibrational mode assignments for acetylene on the ~ 1 and ~ 6 ML Pd/W(211) surfaces are listed in Table 1.

Figure 10 shows HREEL spectra obtained after exposing a ~ 1 ML Pd/W(211) surface at 100 K to 1 L of C_2H_2 (left panel) and C_2D_2 (right panel) and then heating to the indicated temperatures. Most of the features in the spectra obtained at 100 K (Figures 10a and 10e) are consistent with molecularly adsorbed acetylene, as indicated in Table 1. For example, the feature at 780 (600) and 655 (460) cm^{-1} result from symmetric and asymmetric C–H(D) rocking modes, respectively, of molecular C_2H_2 and C_2D_2 . Also, the feature at 1440 (1375)

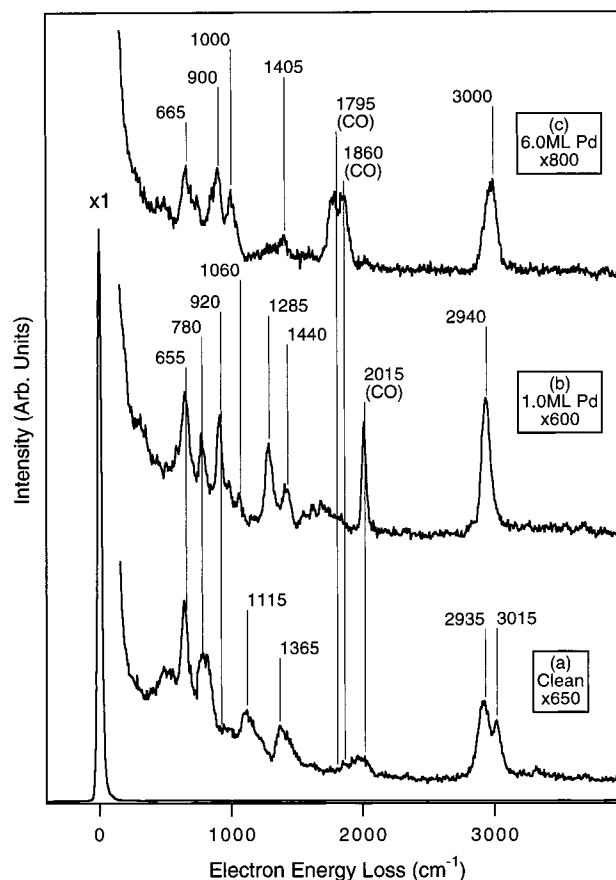


Figure 9. Comparison of HREEL spectra of 1 L of acetylene on clean W(211) and ~ 1 and ~ 6 ML Pd/W(211) at 100 K (a–c), respectively. All spectra were taken in the specular direction with a primary beam energy of 6.0 eV. The surfaces have been preannealed at 700 K for 1 min.

cm^{-1} is assigned to the $\nu(CC)$ feature of molecular C_2H_2 and C_2D_2 on Pd(111)⁹ (cf. Table 1).

The spectra of Figure 10 also show that a fraction of the acetylene decomposes at 100 K. Evidence of this behavior is given by the additional $\nu(CC)$ feature at 1285 (1250) cm^{-1} in Figure 10a (10e), which indicates that another C_2 intermediate is also present on the surface. This C_2 surface intermediate most likely is not strongly perturbed acetylene because such a species would be expected to generate an additional, distinct set of C–H rocking, deformation, and stretching modes, and only one set of modes is observed in Figures 10a and 10e. In contrast to the work of Ormerod et al. for C_2H_2 on Pd(111),⁶⁰ where a vinylidene intermediate was identified, the absence of any $\delta(CH_2)$ or $\delta(CH_3)$ modes in this study (see Table 1) suggests that the C_2 intermediate is not vinyl, vinylidene, or ethynylidyne. Thus, the C_2 intermediate is most likely acetylide (CCH). Interestingly, although the partial dehydrogenation of acetylene to form acetylide should generate surface hydrogen, we could not resolve any Pd–H stretching features, possibly because they may overlap with C–H(D) deformation features. Similar difficulties in observing Pd–H stretching modes have been encountered in previous studies of acetylene on Pd(110).⁴⁴

Figure 10b is quite similar to Figure 10a, suggesting that molecular acetylene and acetylide are stable to 300 K on the ~ 1 ML Pd/W(211) surface. Upon heating to 350 K (Figure 10c), several pronounced changes occur. For example, the feature in the C–H stretching region broadens considerably, with a shoulder appearing at 3045 cm^{-1} . Also, new features appear at 710 and 865 cm^{-1} and the $\rho_s(C-H)$ feature at 780

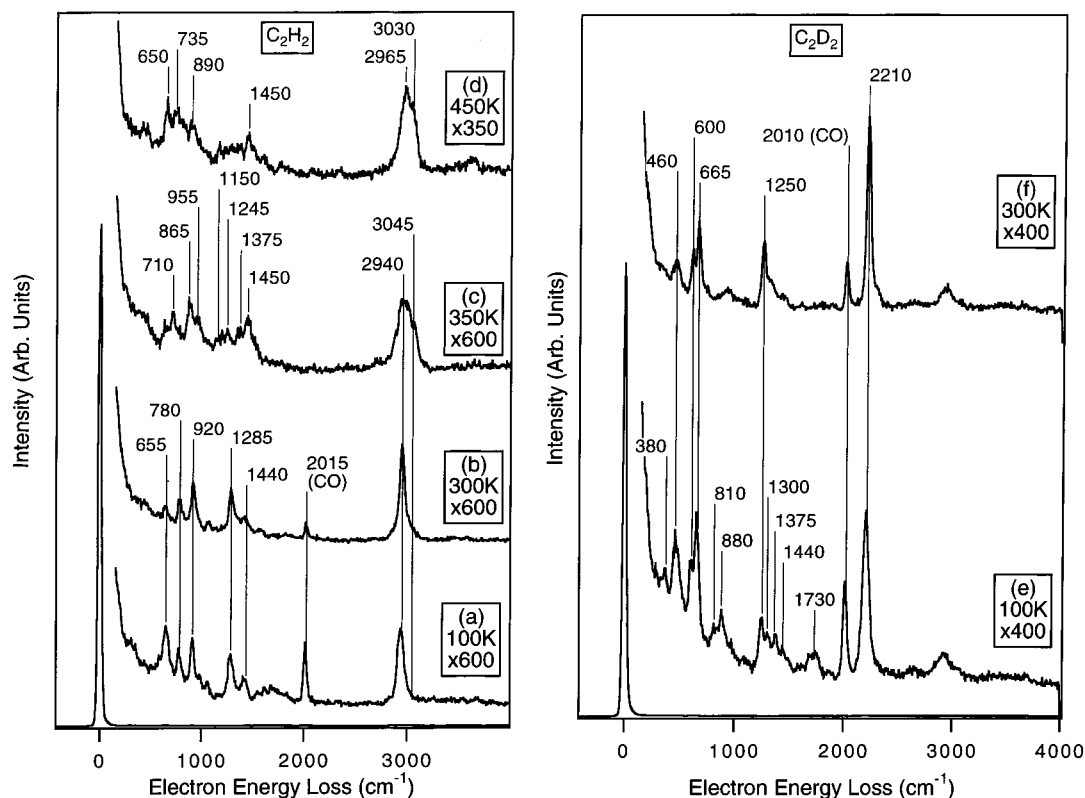


Figure 10. HREEL spectra of (a–d) 1 L of acetylene and (e–f) 1 L of acetylene- d_2 on ~ 1 ML Pd/W(211); obtained as a function of increasing annealing temperature. All annealed surfaces were recooled to 100 K prior to HREELS measurements.

TABLE 1: Vibrational Assignments of Gaseous⁶³ and Chemisorbed Acetylene on Several Metals^{9,23,64} and 1 and 6 ML Pd/W(211)

vibrational assignments (cm^{-1})	gaseous $\text{C}_2\text{H}_2(\text{C}_2\text{D}_2)^{63}$	$\text{C}_2\text{H}_2(\text{C}_2\text{D}_2)$ on Ni(110) ⁶⁴	$\text{C}_2\text{H}_2(\text{C}_2\text{D}_2)$ on Pd(110) ⁶⁴	$\text{C}_2\text{H}_2(\text{C}_2\text{D}_2)$ on Cu(110) ²³	$\text{C}_2\text{H}_2(\text{C}_2\text{D}_2)$ on Pd(111) ⁹	1 L $\text{C}_2\text{H}_2(\text{C}_2\text{D}_2)$ on 1 ML Pd/W(211) at 100 K (this work)	1 L $\text{C}_2\text{H}_2(\text{C}_2\text{D}_2)$ on 6 ML Pd/W(211) at 100 K (this work)
$\nu_s(\text{CH})$	3287 (2427)	2950 (2200)	2990 (2245)	2900 (2190)	2922 (2249)	2940 (2210)	3000 (2210)
$\nu_{as}(\text{CH})$	3374 (2701)						
$\nu(\text{CC})$	1974 (1752)	1350 (1205)	1400 (1274)	1305 (1280)	1402 (1359)	1285 (1250)	1405 (1360)
$\nu(\text{CC})$						1440 (1375)	
$\delta_s(\text{CH})$	729 (539)			940 (680)	1034 (850)	920 (665)	1000 (845)
$\delta_{as}(\text{CH})$	612 (505)			1140 (930)		1060 (810)	
$\rho_s(\text{CH})$	729 (539)	675 (495)	690 (530)		673 (511)	780 (600)	900 (645)
$\rho_{as}(\text{CH})$	612 (505)	910 (685)	915 (700)		872 (621)	655 (460)	665 (480)
$\nu(\text{CM})$		470 (—)	obscured	470 (400)	500 (—)	obscured	obscured

cm^{-1} decreases in relative intensity. Since the TPD results in Figure 5 show that the hydrocarbon reaction products all start to desorb around 350 K, it is instructive to compare the HREEL spectrum obtained at 350 K with the TPD spectra of the reaction products. We begin by considering the TPD spectrum of C_2H_4 , which is the major gas-phase reaction product, as shown by the TPD product distribution histogram in Figure 6. Because we have not performed HREELS investigations of C_2H_4 on the ~ 1 ML Pd/W(211) surface in the current study, we compare Figure 10c with the HREELS studies by Nishijima et al. of C_2H_4 on Pd(110),⁶¹ which has a row-and-trough structure similar to the ~ 1 ML Pd/W(211) surface. Such a comparison reveals that the vibrational features in Figure 10c are consistent with the presence of di- σ -bonded surface ethylene as opposed to a π -bonded ethylene species on Pd(110).⁶¹ In particular, the absence of a $\nu(\text{C}=\text{C})$ mode near 1600 cm^{-1} strongly suggests that ethylene is bonded to the surface in a di- σ -bonded configuration. Other features in Figure 10c can be assigned as follows: $[710, 865 \text{ cm}^{-1}; \rho(\text{CH}_2)]$, $[955 \text{ cm}^{-1}; \omega(\text{CH}_2)]$, $[1150 \text{ cm}^{-1}; \tau(\text{CH}_2)]$, $[1245 \text{ cm}^{-1}; \delta_s(\text{CH}_2)]$, $[1450 \text{ cm}^{-1}; \delta_a(\text{CH}_2)]$, and $[2940 \text{ cm}^{-1}; \nu(\text{CH})]$. Finally, after heating the ~ 1 ML Pd/

W(211) surface to 450 K (Figure 10d), the relative intensities of the vibrational features change slightly. Most importantly, Figure 10d is not characteristic of benzene, as we show below by exposing a ~ 1 ML Pd/W(211) surface to benzene (see discussion of Figure 12 in section 3.2.2). Given that the benzene desorption occurs between 350 and 500 K (Figure 5), the absence of vibrational features of benzene in Figures 10c,d indicates that benzene evolution on the ~ 1 ML Pd/W(211) surface is reaction-limited. In addition, the absence of C_4H_4 vibrational modes on the ~ 1 ML Pd/W(211) surfaces (Figure 10) and the observation of C_4H_6 during TPD (cf. Figure 5) may also indicate a reaction-limited process.

Figure 11 shows HREEL spectra obtained after exposing a ~ 6 ML Pd/W(211) surface to 1 L of acetylene at 100 K and then heating to the indicated temperatures. The spectra obtained between 150 and 250 K (Figures 11b–d) are similar to that obtained at 100 K (Figure 11a), suggesting that molecular acetylene is stable on the ~ 6 ML Pd/W(211) surface at temperatures up to 250 K. Upon heating to 300 K, a pronounced feature appears at 1400 cm^{-1} , with a low-frequency shoulder at 1325 cm^{-1} . A feature also develops at 1225 cm^{-1} . The

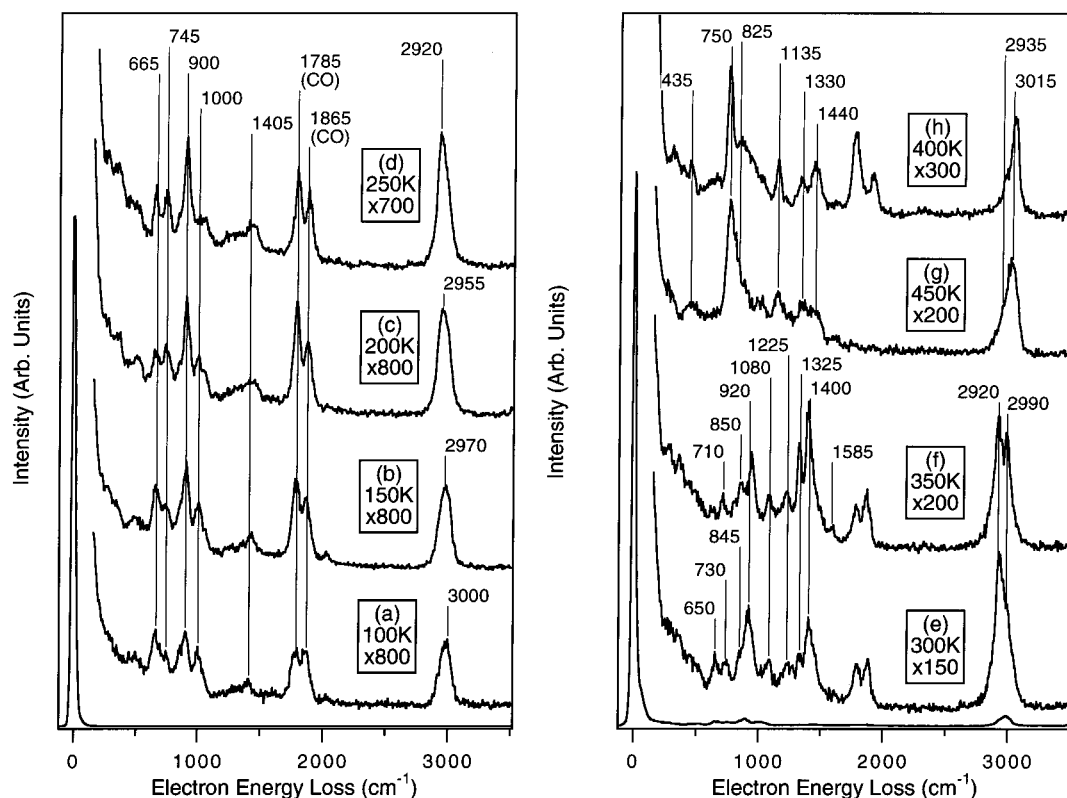


Figure 11. (a–g) HREEL spectra of 1 L of acetylene on ~6 ML Pd/W(211), recorded as a function of increasing annealing temperature. (h) 1 L of chemisorbed benzene on ~6 ML Pd/W(211) annealed to 400 K is shown for comparison with Figure 11g. All annealed surfaces were recooled to 100 K prior to HREELS measurements.

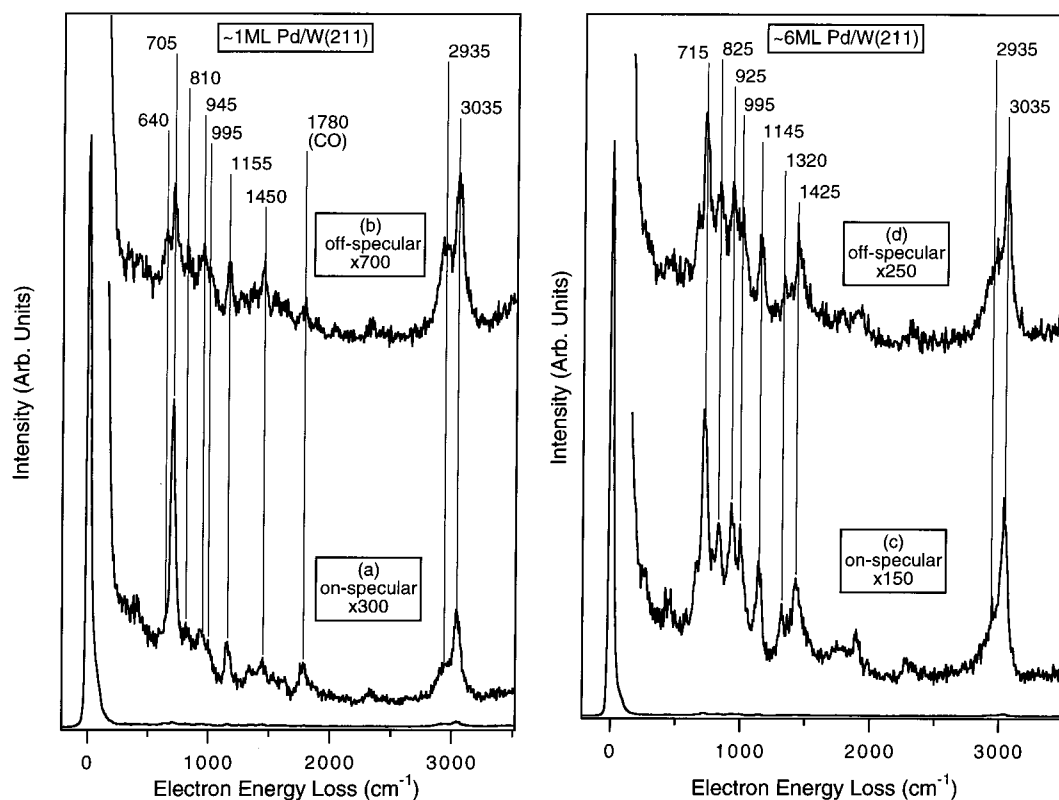


Figure 12. HREEL spectra of 1 L of benzene on (a,b) ~1 ML and (c,d) ~6 ML Pd/W(211) at 100 K in the on-specular and off-specular directions. intensities of the features between 1200 and 1500 cm⁻¹ increase upon heating to 350 K, and a new C–H stretching feature appears at 2990 cm⁻¹. The new features in Figure 11e between 1200 and 1500 cm⁻¹ clearly are not characteristic of acetylene, indicating that acetylene is reacting on the surface to produce

new intermediates. Although we have not performed extensive deuterium-labeling studies to identify the reaction products, the existing evidence indicates that a Pd(C₄H₄) metallocycle is most likely produced on the ~6 ML Pd/W(211) surface at 350 K. This conclusion is based on the following three observations.

TABLE 2: Vibrational Frequencies (cm⁻¹) and Assignments for the Surface Intermediate Formed on the ~6 ML Pd/W(211) Surface at 350 K^a

vibrational assignments (cm ⁻¹)	furan C _{2v} symmetry ⁶⁵			thiophene C _{2v} symmetry ⁶⁶			Pd(C ₄ H ₄) metacycle ⁶		Pd(C ₄ H ₄) metacycle (this work)
	freq		sym	freq		sym	freq	sym	freq
$\nu(\text{CH})$	3167	ν_1	A ₁	3126	ν_1	A ₁	2915	A ₁	2990
$\nu(\text{CH})$	3140	ν_2	A ₁	3098	ν_2	A ₁			2920
ν_{ring}	1556	ν_{14}	B ₁	1507	ν_{14}	B ₁			1585
ν_{ring}	1491	ν_5	A ₁	1409	ν_5	A ₁	1220	A ₁	1400
ν_{ring}	1384	ν_4	A ₁	1360	ν_4	A ₁			1325
$\delta(\text{CH})$	1267	ν_{15}	B ₁	1256	ν_{15}	B ₁	1220	B ₁	1225
$\delta(\text{CH})$	1066	ν_6	A ₁	1083	ν_6	A ₁	1100	A ₁	1080
$\delta(\text{CH})$	995	ν_7	A ₁	1036	ν_7	A ₁	890	A ₁	
ν_{ring}	1140	ν_3	A ₁	839	ν_3	A ₁			850
δ_{ring}	873	ν_{18}	B ₁	751	ν_{18}	B ₁			710
$\gamma(\text{CH})$	745	ν_{19}	B ₂	712	ν_{19}	B ₂	790		

^a The intermediate is most likely a di- σ -metallacyclopentadienyl, as seen by comparisons to structurally related molecules, such as furan and thiophene. The vibrational spectrum of the proposed Pd(C₄H₄) intermediate is also consistent with that of the Pd(C₄H₄) metacycle formed on Pd(111) using a halogenated cyclobutene precursor.⁶ ^b See text for details.

TABLE 3: Vibrational Assignments of Gaseous⁶⁷ and Chemisorbed Benzene on Several Metals^{68–70} 1 and 6 ML Pd/W(211)

vibrational assignments (cm ⁻¹)					1 L C ₆ H ₆ (C ₆ D ₆) on 1 ML Pd/W(211) at 100 K (this work)	1 L C ₆ H ₆ on 6 ML Pd/W(211) at 100 K (this work)	1 L C ₂ H ₂ on 6 ML Pd/W(211) heated to 450 K (this work)	1 L C ₆ H ₆ on 6 ML Pd/W(211) heated to 400 K (this work)
	gaseous C ₆ H ₆ (C ₆ D ₆) ⁶⁷	C ₆ H ₆ (C ₆ D ₆) on Pd(111) ⁶⁸	C ₆ H ₆ (C ₆ D ₆) on Ni(111) ⁶⁹	C ₆ H ₆ (C ₆ D ₆) on Pd(110) ⁷⁰				
$\nu(\text{CH})$ ν_1	3047 (2265)	2990 (2230)	3020 (2250)	3050 (2320)	3035 (2260)	3035	3015	3030
$\nu(\text{CH})$					2935	2935	2935	2935
$\nu(\text{CC})$ ν_{16}	1596 (1552)			1580 (1550)	obscured			
$\nu(\text{CC}) + \delta(\text{CC})$ ν_{13}	1486 (1335)	1410 (1355)	1420 (1360)	1460 (1420)	1450 (1440)	1425	1440	1440
$\delta(\text{CC})$ ν_9	1310 (1286)		1320 (1225)	1340 (1230)		1320	1330	1330
$\delta(\text{CH})$ ν_{10}	1150 (824)	1100 (830)	1110 (820)	1150 (870)	1155 (845)	1145	1135	1135
$\delta(\text{CH})$ ν_{14}	1038 (816)		845 (645)					
$\nu(\text{CC})$ ν_2	992 (943)	(830)	845 (820)	890 (870)	945 (915)	925		
$\gamma(\text{CH})$ ν_{11}	849 (662)	810 (640)		890 (680)	810 (630)	825	825	825
$\gamma(\text{CH})$ ν_4	673 (497)	720 (525)	745 (540)	705 (505)	705 (515)	715	750	750
$\nu(\text{CM})$		265 (270)		350 (340)	385 (380)	430	435	435

First, the vibrational spectrum in Figure 11f agrees well with the infrared spectra of furan and thiophene (cf. Table 2), two molecules which are structurally similar to the proposed Pd(C₄H₄) metacycle. Second, Figure 11f is qualitatively consistent (cf. Table 2) with the HREEL spectrum of a Pd-(C₄H₄) metacycle formed by the dissociative adsorption of *cis*-3,4-dichlorocyclobutene on Pd(111).⁶ Finally, as discussed below, the spectrum in Figure 11f changes upon heating to become characteristic of benzene (cf. Figures 11g and 11h). Since alkyne cyclotrimerization to form benzene or substituted benzenes is believed to proceed via a metacycle intermediate,⁶² it is reasonable to expect a Pd(C₄H₄) intermediate on the surface prior to the formation of benzene.

As shown in Figure 11, after heating to 450 K, the corresponding HREEL spectrum (Figure 11g) is nearly identical to that obtained after directly dosing benzene on a ~6 ML Pd/W(211) surface and then heating to 400 K (Figure 11h), suggesting that the Pd(C₄H₄) metacycles are converted to surface benzene. However, unlike the case for the ~1 ML Pd/W(211) surface, the production of benzene on ~6 ML Pd/W(211) is desorption-limited. An assignment of the vibrational features in Figures 11g and 11h to chemisorbed benzene is given in Table 3.

3.2.2. Benzene on Pd/W(211) Surfaces. To investigate the bonding of benzene on the ~1 and ~6 ML Pd/W(211) surfaces further, benzene was directly chemisorbed on both surfaces at 100 K. Figure 12 shows on- and off-specular HREEL spectra obtained after exposing the ~1 ML Pd/W(211) surface (left panel) and the ~6 ML Pd/W(211) surface (right panel) to 1 L of benzene. There are several noteworthy aspects about the spectra shown in Figure 12. First, a comparison of the

vibrational features in Figure 12 with those of gas-phase benzene (cf. Table 3) indicates that benzene adsorbs molecularly on both surfaces. Second, although the spectra are consistent with the molecular adsorption of benzene, the presence of softened C–H modes (at 2935 cm⁻¹ for benzene on either surface) show that the surface–benzene interaction is strong enough to perturb the C–H modes. Third, the spectra show that benzene is bonded nearly parallel to the ~1 ML Pd/W(211) surface, but the average orientation of benzene is isotropic on the ~6 ML Pd/W(211) surface. This behavior is determined by comparing the relative intensities of the $\gamma(\text{CH})$ out-of-plane deformation mode at ~705–715 cm⁻¹ (the ν_4 mode in Herzberg Notation)⁶³ in the on- and off-specular spectra of benzene on each surface. Such a comparison reveals a strong angle-dependent variation in the relative intensity of the ν_4 mode for benzene on the ~1 ML Pd/W(211) surface, but essentially no such variation is observed in the spectra for benzene on the ~6 ML Pd/W(211) surface. Since the ν_4 mode has a dynamic dipole which is perpendicular to the plane of the benzene molecule, a strong angle-dependent variation in the intensity of the ν_4 mode of benzene on the ~1 ML Pd/W(211) surface indicates that the benzene molecule is essentially parallel to the surface. Using similar reasoning, one concludes that the benzene is not parallel to the macroscopic surface plane on ~6 ML Pd/W(211). This behavior may result from the adsorption of benzene in different bonding configurations on the surface of the annealed polycrystalline 6 ML film.

The observation of a strong angular dependence of the HREEL spectra for benzene on the 1 ML Pd/W(211) surface is somewhat intriguing, since similar experiments in the preceding paper showed a complete lack of angular dependence for benzene on a clean W(211) surface. On the basis of the STM

results, both clean W(211) and the 1 ML Pd/W(211) are characterized by a row-and-trough surface structure. At present we do not understand the origin of the different angular dependence in the HREELS measurements of benzene on the two surfaces. More structural-sensitive tools, such as the polarization-dependent near-edge X-ray absorption fine structure measurements, are needed to obtain a better understanding regarding the adsorption geometry of benzene on the two surfaces.

Finally, the HREEL spectra of chemisorbed benzene on Pd/W(211) at 100 K (Figure 12) are slightly different from those obtained after annealing the surface to 400 K (see, for example, Figure 11h). Although the ν_4 features (Table 3) are dominant at both temperatures, the vibrational features are not as well-resolved after heating to 400 K and the ν_4 features shift to higher frequency. Such behavior could result from a stronger interaction between reactively formed benzene and the Pd/W(211) surface at 400 K than between chemisorbed benzene and the surface at 100 K.

4. Conclusions

The unique reactivity of the ~ 1.0 ML Pd/W(211) surface, as compared to the clean W(211) and multilayer Pd/W(211) surface, is demonstrated by both TPD and HREELS studies. For example, the evolution of benzene from the ~ 1.0 ML Pd/W(211) surface shows three desorption features at 340, 390, and 430 K, while no benzene desorption is observed from the clean W(211) surface. In addition, the observation of a C_4H_6 species in TPD measurements strongly suggests that a C_4H_4 surface intermediate is involved in the formation of benzene. Moreover, TPD and HREELS have shown the desorption of reactively formed benzene to be reaction-rate-limited on the ~ 1 ML Pd/W(211) surface. Furthermore, HREELS results indicate that the adsorption and the subsequent reaction of acetylene are qualitatively different on the ~ 1.0 ML Pd/W(211) surface and the multilayer Pd/W(211) surface. In addition, the HREELS results on multilayer Pd/W(211) also reveal the presence of a Pd(C_4H_4) metallocycle, which is believed to subsequently couple with acetylene to form surface benzene. Interestingly, the reactively produced benzene can be retained on the ~ 6 ML Pd/W(211) surface after formation; in contrast, reactively formed benzene appears to desorb efficiently from monolayer Pd/W(211) at the temperatures where it is formed. More detailed studies are needed to understand the different reactivities of benzene on the monolayer and multilayer Pd/W(211) surfaces.

The results presented here for Pd/W(211) provide a clear demonstration that bimetallics change surface activity. For instance, acetylene cyclization does not occur on the clean W(211) surface while the adsorption of a single monolayer of Pd catalyzes the reaction. Furthermore, although the Pd(110) and Pd/W(211) surfaces both have row-and-trough structures, the Pd(110) surface does not catalyze the cyclization pathway with significant yields nor the desorption of C_4H_6 at all, unlike the Pd/W(211) surface. This behavior indicates that the presence of the W substrate very likely changes the electronic structure of the Pd adlayer, perhaps imitating the electronic structure of Cu(110) rather than that of Pd(110). To understand further the correlation between the morphology and chemical reactivity of these morphologically unstable surfaces, investigations using acetylene as a probing molecule will be performed on planar and faceted Pd/W(111) surfaces.

Acknowledgment. This work has been supported in part by the Division of Chemical Sciences, U.S. Department of Energy.

References and Notes

- (1) Eng, J., Jr.; Chen, J. G.; Abdelrehim, I. M.; Madey, T. E. *J. Phys. Chem. B* **1998**, *102*, 9687.
- (2) Tysoe, W. T.; Nyberg, G. L.; Lambert, R. M. *J. Chem. Soc., Chem. Commun.* **1983**, 623.
- (3) Tysoe, W. T.; Nyberg, G. L.; Lambert, R. M. *Surf. Sci.* **1983**, *135*, 128.
- (4) Sesselmann, W.; Woratschek, B.; Ertl, G.; Küppers, J.; Haberland, H. *Surf. Sci.* **1983**, *130*, 245.
- (5) Gentle, T. M.; Muetterties, E. L. *J. Phys. Chem.* **1983**, *87*, 2469.
- (6) Patterson, C. H.; Mundenar, J. M.; Timbrell, P. Y.; Gellman, A. J.; Lambert, R. M. *Surf. Sci.* **1989**, *208*, 93.
- (7) Marchon, B. *Surf. Sci.* **1985**, *162*, 382.
- (8) Kesmodel, L. L.; Waddill, G. D.; Gates, J. A. *Surf. Sci.* **1984**, *138*, 464.
- (9) Gates, J. A.; Kesmodel, L. L. *J. Chem. Phys.* **1982**, *76* (8), 4281.
- (10) Rucker, T. G.; Logan, M. A.; Gentle, T. M.; Muetterties, E. L.; Somorjai, G. A. *J. Phys. Chem.* **1986**, *90*, 2703–2708.
- (11) Vollhardt, K. P. C. *Acc. Chem. Res.* **1977**, *10*, 1.
- (12) Maitlis, P. M. *Acc. Chem. Res.* **1976**, *9*, 93.
- (13) Hoffman, H.; Zaera, F.; Ormerod, R. M.; Lambert, R. M.; Yao, J. M.; Saldin, D. K.; Wang, L. P.; Bennett, D. W.; Tysoe, W. T. *Surf. Sci.* **1992**, *268*, 1.
- (14) Gentle, T. M.; Tsai, C. T.; Walley, K. P.; Gellman, A. J. *Catal. Lett.* **1989**, *2*, 19.
- (15) Gellman, A. J. *J. Am. Chem. Soc.* **1991**, *113*, 4435.
- (16) Gellman, A. J. *Langmuir* **1991**, *7*, 827.
- (17) Gellman, A. J. *J. Phys. Chem.* **1992**, *96*, 790.
- (18) Ormerod, R. M.; Lambert, R. M. *Catal. Lett.* **1990**, *6*, 121–130.
- (19) Abdelrehim, I. M.; Thornburg, N. A.; Sloan, J. T.; Land, D. P. *Surf. Sci. Lett.* **1993**, *298*, L169.
- (20) Gates, J. A.; Kesmodel, L. L. *Surf. Sci.* **1983**, *124*, 68.
- (21) Logan, M. A.; Rucker, T. G.; Gentle, T. M.; Muetterties, E. L.; Somorjai, G. A. *J. Phys. Chem.* **1986**, *90*, 2709.
- (22) Lambert, R. M.; Ormerod, R. M. Tricyclization and Heterocyclization Reactions of Ethyne over Well-Defined Palladium Surfaces. In *Springer Series in Surface Science, Surface Reactions*; Madix, R. J., Ed.; Springer-Verlag: Berlin, 1994; Vol. 34, pp 89–134.
- (23) Avery, N. R. *J. Am. Chem. Soc.* **1985**, *107*, 6711.
- (24) Lomas, J. R.; Baddeley, C. J.; Tikhov, M. S.; Lambert, R. M. *Langmuir* **1995**, *11*, 3048.
- (25) Patterson, C. H.; Lambert, R. M. *J. Phys. Chem.* **1988**, *92*, 1266.
- (26) Patterson, C. H.; Lambert, R. M. *J. Am. Chem. Soc.* **1988**, *110*, 6871.
- (27) Abdelrehim, I. M.; Thornburg, N. A.; Sloan, J. T.; Caldwell, T. E.; Land, D. P. *J. Am. Chem. Soc.* **1995**, *117*, 9509.
- (28) Abdelrehim, I. M.; Caldwell, T. E.; Land, D. P. *J. Phys. Chem.* **1996**, *100*, 10265.
- (29) Ormerod, R. M.; Lambert, R. M.; Bennett, D. W.; Tysoe, W. T. *Surf. Sci.* **1995**, *330*, 1.
- (30) Lee, A. F.; Baddeley, C. J.; Hardacre, C.; Lambert, R. M. *J. Am. Chem. Soc.* **1995**, *117*, 7719.
- (31) Ormerod, R. M.; Lambert, R. M.; Hoffman, H.; Zaera, F.; Yao, J. M.; Saldin, D. K.; Wang, L. P.; Bennett, D. W.; Tysoe, W. T. *Surf. Sci.* **1993**, *295*, 277.
- (32) Pacchioni, G.; Lambert, R. M. *Surf. Sci.* **1994**, *304*, 208.
- (33) Ramirez-Cuesta, A.; Zgrablich, G.; Tysoe, W. T. *Surf. Sci.* **1995**, *340*, 109.
- (34) Abdelrehim, I. M.; Pelhos, K.; Eng, J., Jr.; Chen, J. G.; Madey, T. E. *J. Mol. Catal. A: Chem.* **1998**, *131*, 107.
- (35) Bertolini, J. C.; Massardier, J.; Dalmay-Imelik, G. *J. Chem. Soc., Faraday Trans. 1* **1978**, *74*, 1720.
- (36) Ormerod, R. M.; Lambert, R. M. *J. Chem. Soc., Chem. Commun.* **1990**, 1421.
- (37) Lee, A. F.; Baddeley, C. J.; Hardacre, C.; Ormerod, R. M.; Lambert, R. M. *J. Phys. Chem.* **1995**, *99*, 6096.
- (38) Ormerod, R. M.; Baddeley, C. J.; Lambert, R. M. *Surf. Sci. Lett.* **1991**, *259*, L709.
- (39) Baddeley, C. J.; Ormerod, R. M.; Stephenson, A. W.; Lambert, R. M. *J. Phys. Chem.* **1995**, *99*, 5146.
- (40) Baddeley, C. J.; Tikhov, M.; Hardacre, C.; Lomas, J. R.; Lambert, R. M. *J. Phys. Chem.* **1996**, *100*, 2189.
- (41) Heitzinger, J. M.; Gebhard, S. C.; Koel, B. E. *J. Phys. Chem.* **1993**, *97*, 5327.
- (42) Heitzinger, J. M. Ph.D. Thesis, University of Southern California, 1993.
- (43) Xu, C.; Peck, J. W.; Koel, B. E. *J. Am. Chem. Soc.* **1993**, *115*, 751–755.
- (44) Yoshinobu, J.; Sekitani, T.; Onchi, M.; Nishijima, M. *J. Phys. Chem.* **1990**, *94*, 4269.
- (45) Ormerod, R. M.; Lambert, R. M. *J. Phys. Chem.* **1992**, *96*, 8111.
- (46) Sinfelt, J. H. *Bimetallic Catalysts*; Wiley: New York, 1983.

- (47) Campbell, C. T. *Annu. Rev. Phys. Chem.* **1990**, *41*, 775–837.
- (48) Guan, J.; Campbell, R. A.; Madey, T. E. *Surf. Sci.* **1995**, *341*, 311.
- (49) Nien, C.-H.; Madey, T. E. *Surf. Sci.* **1997**, *380*, L527.
- (50) Madey, T. E.; Guan, J.; Dong, C.-Z.; Shivaprasad, S. M. *Surf. Sci.* **1993**, *287/288*, 826.
- (51) Guan, J.; Campbell, R. A.; Madey, T. E. *J. Vac. Sci. Technol.* **1995**, *13*, 1484.
- (52) Madey, T. E.; Guan, J.; Nien, C.-H.; Dong, C. Z.; Tao, H.-S.; Campbell, R. A. *Surf. Rev. Lett.* **1996**, *3*, 1315.
- (53) Campbell, R. A.; Guan, J.; Madey, T. E. *Catal. Lett.* **1994**, *27*, 273.
- (54) Dong, C.; Zhang, L.; Diebold, U.; Madey, T. E. *Surf. Sci.* **1995**, *322*, 221.
- (55) Frühberger, B.; Chen, J. G. *Surf. Sci.* **1995**, *342*, 38.
- (56) Pierce, K. G.; Barteau, M. A. *J. Phys. Chem.* **1994**, *98*, 3882.
- (57) Nakao, F. *Vacuum* **1975**, *25*, 431.
- (58) Kolodziej, J. J.; Pelhos, K.; Abdelrehim, I. M.; Keister, J.; Rowe, J. E.; Madey, T. E. *Prog. Surf. Sci.* **1998**, in press.
- (59) Pelhos, K.; Abdelrehim, I. M.; Madey, T. E. Manuscript in preparation.
- (60) Ormerod, R. M.; Lambert, R. M.; Hoffman, H.; Zaera, F.; Wang, L. P.; Bennett, D. W.; Tysoc, W. T. *J. Phys. Chem.* **1994**, *98*, 2134.
- (61) Nishijima, M.; Yoshinobu, J.; Sekitani, T.; Onchi, M. *J. Chem. Phys.* **1990**, *90* (9), 5114.
- (62) Collman, J. P.; Hegedus, L. S. In *Principles and Applications of Organotransition Metal Chemistry*; Kelly, A., Ed.; University Science Books: Mill Valley, CA, 1980; p 525.
- (63) Herzberg, G. In *Molecular Spectra and Molecular Structure, Vol. II: Infrared and Raman Spectra of Polyatomic Molecules*; Van Nostrand Reinhold Company Inc.: New York, 1945.
- (64) Bandy, B. J.; Chesters, M. A.; Pemble, M. E.; McDougall, G. S. *Surf. Sci.* **1984**, *139*, 87.
- (65) Rico, M.; Barrachina, M.; Orza, J. M. *J. Mol. Spectrosc.* **1967**, *24*, 133.
- (66) Rico, M.; Orza, J. M.; Morcillo, J. *Spectrochim. Acta* **1965**, *21*, 689.
- (67) Shimanouchi, T. In *Tables of Molecular Vibrational Frequencies*; National Bureau of Standards: Washington, D.C., 1972; Vol. II (39).
- (68) Waddill, G. D.; Kesmodel, L. L. *Phys. Rev. B* **1985**, *31*, 4940.
- (69) Bertolini, J. C.; Rousseau, J. *Surf. Sci.* **1979**, *89*, 467.
- (70) Fujisawa, T.; Sekitani, T.; Morikawa, Y.; Nishijima, M. *J. Phys. Chem.* **1991**, *95*, 7415.